

Preparation and characterization of cellulose acetate and lithium nitrate for advanced electrochemical devices

S. Monisha^{1,2} · T. Mathavan¹ · S. Selvasekarapandian² · A. Milton Franklin Benial¹ · M. Prema latha^{1,2}

Received: 31 August 2016 / Revised: 1 October 2016 / Accepted: 27 October 2016 / Published online: 14 November 2016
© Springer-Verlag Berlin Heidelberg 2016

Abstract Environmental research has the objective of finding solutions to environmental degradation. To this aim, an optimized solid bio-polymer electrolyte (BPE) based on cellulose acetate (CA) with lithium nitrate (LiNO_3) has been developed to achieve the possible energy storage Li-ion batteries. CA is one of the natural polymers with very good film forming capacity. The widespread use of CA is attributed to the availability of renewable resources, non-toxic nature, low cost, and bio-compatible material. Here, we demonstrate an extremely simplest process of solution-casting technique for the development of BPE by incorporating various LiNO_3 compositions (wt.%) with bio-polymer material CA. The crystalline nature of the CA with LiNO_3 has been analyzed by X-ray diffraction (XRD) measurement. The bio-polymer-salt complex formation and the biopolymer-proton interactions have been investigated through Fourier transform infrared (FTIR) spectroscopy. Electrochemical impedance spectroscopy has been used to examine the ionic conductivity of the BPEs at room temperature (303 K). The highest ionic conductivity of $1.93 \times 10^{-3} \text{ S/cm}$ has been achieved for 50CA/50 LiNO_3 polymer electrolyte. Electrochemical studies show that highest BPE has high electrochemical stability windows. The conducting species is found to be Li^+ ion, which has been confirmed by transference number measurement (TNM). Primary lithium battery with discharge profile has

been constructed for 50CA/50 LiNO_3 . This research will help to identify a new lithium ion membrane for battery technology and other electrochemical device applications.

Keywords Biopolymer electrolyte · Cellulose acetate · Lithium nitrate · Conductivity · Electrochemical stability · Primary battery

Introduction

Nowadays, there is a worldwide demand for the development of sustainable, safe, and environmentally friendly energy resources. One key to realize this demand is the development of new solid polymer electrolytes (SPEs). Lithium batteries based on SPEs have many advantages over the liquid counterparts, in which they are flexible, conform to any battery shape, eliminate the need for a separator, and can improve the safety and stability of batteries due to their non-leakage and non-reactive characteristics [1]. However, the main drawback on practical use of solvent-free polymer electrolyte is low ionic conductivity at room temperature. To overcome the above issue, some of the researchers approach includes polymer blending, addition of inorganic fillers, and use of plasticizers [2–4]. Tiankhon et al. have tried to improve the ionic conductivity by offering the polymer blending of poly(vinylidene fluoride)-poly(methyl methacrylate)-grafted natural rubber (PVDF-MG49) doped with lithium trifluoromethanesulfonate (LiCF_3SO_3). But the results showed low ionic conductivity of $3.25 \times 10^{-4} \text{ S/cm}$ [2]. New solid polymer electrolyte based on poly(ethylene glycol) (PEO)-lithium 4,5-dicyano-2-(trifluoromethyl) imidazolidine (LiTDI) and SN as plasticizer has been developed for lithium batteries, which exhibit the ionic conductivity value of $2.83 \times 10^{-5} \text{ S/cm}$ [3]. Influence of TiO_2 nanoparticles on

✉ T. Mathavan
tjmathavan@gmail.com

¹ Research Department of Physics, N.M.S.S. Vellaichamy Nadar College, Madurai, Tamil Nadu 625019, India

² Materials Research Center, Coimbatore, Tamil Nadu 641 045, India

PEO-LiClO₄ polymer electrolytes exhibits maximum conductivity of 1.40×10^{-4} S/cm [4]. The above authors exhibit the ionic conductivity of order 10^{-4} S/cm by polymer blending through addition of inorganic fillers and plasticizers. In this paper, CA/LiNO₃ BPE gives better ionic conductivity of order 10^{-3} S/cm in single polymer material complex doped with salt, which gives a breakthrough to the development of solid-state electrochemical devices such as solid-state batteries, fuel cells, chemical sensors, supercapacitor, and electrochromic windows [5].

Recently, researchers focused on the use of biodegradable materials (chitosan, corn starch, and agar) as SPEs to address the environmental crises [6–8]. Biopolymer-based electrolytes have been proven to possess great thermal stability, high mechanical property, sufficient electrochemical stability, and high ionic conductivity [7, 9–11]. As a result, natural polymer cellulose acetate (CA) has been chosen to build up the solid polymer membrane. CA has been widely used in textiles, plastic industries, cigarette filters and drug delivery system. It has other credentials such as abundance, non-toxic nature, low cost, and biodegradability. CA has polar functional groups in the main polymer chain, which has high affinity towards lithium ion. However, the main obstacle of CA membrane is high crystalline nature, which proves the CA membrane to be insulated. To overcome the above issue, ionic salts are embedded/incorporated in cellulose acetate [12, 13].

Salt as ion provider is an important constituent of an electrolyte as it gives strong influence on the electrolyte's properties such as conductivity, amorphousness, and thermal stability. Many authors report the use of ammonium salts in the preparation of SPEs. But lithium-based ionic salts is the most preferred one having small size of lithium ions (Li⁺), which provides high gravimetric Coulombic density [14, 15]. This type of ionic salt, such as lithium nitrate (LiNO₃) is of special interest due to its electronegativity and delocalization of charge [12]. Research on CA-based lithium salts have been studied extensively by Ramesh et al., Selvakumar et al., and Abidin et al., respectively [12, 13, 16, 17]. However, there is no work related to CA-based LiNO₃ for electrochemical application. Recently, Kingslin and coworkers proposed a lithium ion conducting blend polymer electrolyte based on poly(vinyl alcohol)-poly(acrylonitrile) (PVA-PAN) doped with lithium nitrate [18]. The weak coordination in presence of salt LiNO₃ makes possible incorporation of ion with the polymer CA and reduces the degree of crystallinity in CA, which leads to increase the ionic conduction.

In this work, we investigate the effect of LiNO₃ of different ratios in the bio polymer electrolyte (BPE) system with the aim of obtaining improved ionic conductivities compared with pure CA. As in this research, the initial approach to suppress the high crystallinity is done by the dissociation of LiNO₃ in CA matrix forming free ions, which could give high ionic conductivities to BPE films. These films have been

characterized by XRD, FTIR, impedance spectroscopy, and linear sweep voltammetry. Furthermore, the ionic transference number by wagners DC polarization method and primary lithium battery for highest conducting sample has been estimated.

Materials and methods

The polymer cellulose acetate (Sigma Aldrich, product code 1001345528) and salt LiNO₃ are used as a raw material in this study. Dimethyl formamide (DMF) has been used as a solvent. The BPE CA doped with different mole percent of LiNO₃ such as 90CA/10LiNO₃, 80CA/20LiNO₃, 70CA/30LiNO₃, 60CA/40LiNO₃, 50CA/50LiNO₃, and 40CA/60LiNO₃ have been prepared by solution casting technique. The mixture of CA and LiNO₃ has been stirred continuously with magnetic stirrer for several hours to obtain homogeneous solution. The solution is then cast in Petri dishes and samples are vacuum dried at 60 °C. The obtained free standing transparent films are taken for further characterization.

Measurements

X-ray diffraction spectra of the prepared BPEs have been carried out by Philips X'pert PRO diffractometer, where X-rays of 1.5406 Å wavelengths were generated by a Cu K α source. The 2 θ angle has been varied from 10° to 80°. FTIR spectrum has been recorded for samples using BRUCKER spectrophotometer in the range 400–4000 cm⁻¹. The impedance measurements have been carried out using HIOKI 3532–50 LCR HITESTER from room temperature to 343 K in the frequency range of 42 Hz to 1 MHz. The measuring BPE films have been sandwiched between two stainless steel electrodes of a conductivity cell. The film with well known thickness (0.22–0.66 μ m) has been measured using micrometer screw gauge. Transference number measurement has been performed using dc polarization method. The dc current is monitored as a function of time on the application of fixed dc voltage (1.5 V) across the sample mounted between two stainless steel electrodes. Primary lithium battery using the membrane with the highest ionic conductivity as electrolyte with the configuration Zn + ZnSO₄.7H₂O/50CA/50LiNO₃/PbO₂ + V₂O₅ has been constructed. The open circuit voltage and discharge characteristics have been reported.

Results and discussion

X-ray diffraction analysis

The changes in the structural property of the BPEs have been investigated by XRD analysis. XRD studies have been carried out for pure CA, 60CA/40LiNO₃, 50CA/50LiNO₃, and

40CA/60LiNO₃ electrolyte films and the diffraction pattern are shown in Fig. 1. The peaks observed at $2\theta = 13^\circ$, 18° , and 27° are the characteristic crystalline peaks of pure CA (Fig. 1a) [12, 13]. The decrease in the intensity of characteristic diffraction peaks are seen with the incorporation of LiNO₃ (Fig. 1b, c), and it clearly indicates that the addition of LiNO₃ to the polymer matrix disrupts the ordering of polymer chain. The disruption in the polymer chain with the addition of LiNO₃ is due to the interaction of lithium ion with the functional group of CA. The increase in salt concentration of LiNO₃ to 50 mol% increases the amorphous nature of BPE. The maximum amorphous nature has been observed for the sample 50CA/50NH₄NO₃. The conductivity of a polymer electrolyte is usually enhanced by an increase in the magnitude of amorphous phase. This leads the polymer chain more flexible, which results in an enhancement of segmental motion in the polymer [19]. XRD results are well consistent with the electrical measurement. None of the peaks pertaining to LiNO₃ salts appear in the XRD pattern of BPE, indicating the complete dissociation of the salt in the polymer matrix. Moreover, beyond the addition of 40 mol% LiNO₃, the salt gets recrystallizes, which reduces the number of charge carriers and the overall ionic conduction of the BPEs (Fig. 1d) [20].

Fourier transform infrared spectroscopy analysis

The sensitivity to molecular and structural changes in BPEs has been detected from FTIR spectra. In this work, FTIR spectroscopy has been used to probe the interaction and complexation between CA and LiNO₃. Figure 2 represents the FTIR spectra for pure CA and CA-LiNO₃ complex of various compositions in the wavenumber region from 800 to 4000 cm⁻¹. In Fig. 2a, the

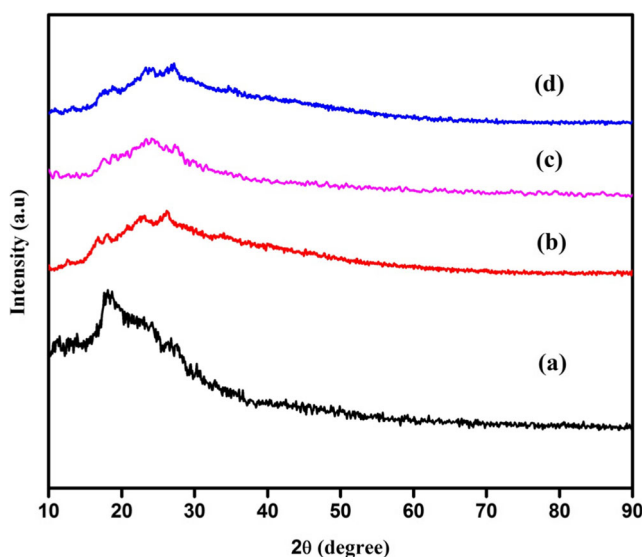


Fig. 1 XRD patterns of *a* pure CA, *b* 60CA/40LiNO₃, *c* 50CA/50LiNO₃, and *d* 40CA/60LiNO₃ BPEs

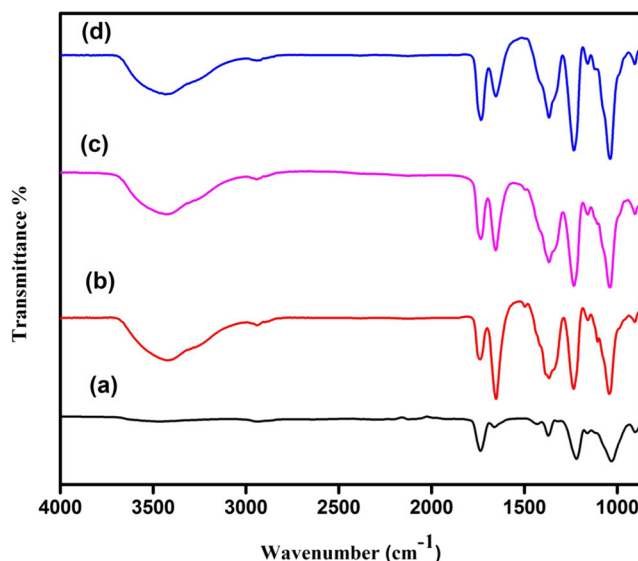


Fig. 2 FTIR spectra of *a* pure CA, *b* 60CA/40LiNO₃, *c* 50CA/50LiNO₃, and *d* 40CA/60LiNO₃ BPEs

detected peaks for pure CA are CH₂ rocking, C–O–C stretching, C–O stretching, CH₂ bending, and C=O symmetric stretching, respectively, at bands 908, 1030, 1219, 1371, and 1736 cm⁻¹ [12, 13]. When the salt concentration is introduced, the changes in intensity, shape and position of the bands are observed. This implies that the complex reaction has been occurred at oxygen from ester group [21]. The shifting in the vibrational peaks and the corresponding assignments are listed in Table 1.

Figure 2 indicates that the addition of LiNO₃ to pure CA shifts the carbonyl group (C=O) stretching vibration, which implies that strong intermolecular interaction is between lithium ion from doping salts and oxygen atoms resulting in polymer salt complexes. The oxygen atoms from CA carbonyl group are expected to act as electron donor atoms and they form coordinate bond with lithium ion from doping salts [22]. The shift in stretching modes of the carbonyl bonds are due to pyrrolidine rings, which have been seen from peaks in the region 1649–1663 cm⁻¹. According to Kumutha et al., this band corresponds to $Li^+ \rightarrow O=C$ interaction [23]. In addition, the peak evolves at 1371 cm⁻¹ and its intensity increases with salt concentration. This strong absorption band has been ascribed to CH₂ bending of NO₃⁻ anion. The increases in the characteristic band of nitrate group demonstrate that LiNO₃ phase has been present in all sample compositions [24]. The broad peak corresponding to hydroxyl group (OH) has been observed and increases with salt concentration, which is due to the hygroscopic nature of lithium salt at around 3420 cm⁻¹ [25].

The conduction mechanism of CA/LiNO₃ complex in lithium ion battery can be illustrated in Scheme 1. From Scheme 1, the coordination and hydrogen bonding interaction between CA and LiNO₃ implies that the ions are mobile in the system. Ion mobility is important in an electrolyte system as high mobility will favor to high ionic conductivity. This suggests

Table 1 Vibrational peaks and assignments of pure CA, 60CA/40LiNO₃, 50CA/50LiNO₃, and 40CA/60LiNO₃ BPEs

Pure CA (cm ⁻¹)	60CA/40LiNO ₃ (cm ⁻¹)	50CA/50LiNO ₃ (cm ⁻¹)	40CA/60LiNO ₃ (cm ⁻¹)	Assignments
908	900	903	903	CH ₂ rocking
1030	1040	1036	1043	C–O–C stretching of pyrose ring
1219	1232	1235	1225	C–O stretching
1371	1365	1371	1365	CH ₂ in plane bending
1736	1737	1733	1737	C=O symmetric stretching

that LiNO₃ has the potential to function as the charge carrier in the system. A conduction pathway has been proposed to be formed as there will be a weakly bound of Li⁺ ion, which can be easily dissociated under the influence of electric field. This Li⁺ ion can hop through the coordinating site of C=O of host polymer and the conduction takes place [26, 27].

Thus, the spectral analysis confirms the complexation and interaction between biopolymer CA and lithium salt LiNO₃.

Ionic conductivity study

Impedance spectroscopy is relatively new and powerful method for understanding the ion conduction mechanism/ion dynamics of the polymer material. Figure 3 shows the complex impedance plot (plot between real and imaginary parts of impedance) for the prepared BPEs at room temperature containing different weight percentage of LiNO₃. In Fig. 3, the observed intercept of plots in the high frequency semicircular region has been associated with the ionic conductivity process in the bulk of the polymer electrolytes. This has been equivalent to the parallel combination of bulk resistance and bulk capacitance. Whereas the low frequency spike has been

attributed to the blocking double layer capacitance near the electrode/electrolyte interface formed by ion migration [3].

From Fig. 3, it is also apparent that increase in salt concentration (10 to 60 wt.%) decrease the semicircular region and only the slanted spike at high frequency region has been observed. The disappearance of semicircular portion in the impedance curve leads to a conclusion that the current carriers are ions and this leads one to further conclude that the total conductivity is mainly the result of ion conduction [28]. The equivalent circuit has been shown in Fig. 3. EIS parameters have been obtained by using EQ software program [29, 30], where the resistance value of pure CA was obtained as $61.2 \times 10^3 \Omega$, whereas for 10–50 mol% of LiNO₃ doped with CA polymer electrolyte, the value of resistance has decreased from 1512 to 14 Ω . The constant phase element (CPE) value for pure CA was obtained as $2.66 \times 10^4 \mu\text{F}$. The LiNO₃ doped with CA polymer electrolyte have CPE values in the range of 0.0026 to 2.45 μF . The highest conducting polymer electrolyte 50CA/50LiNO₃ has $R_b = 14 \Omega$ and CPE = 2.45 μF .

The ionic conductivity (σ) of the polymer electrolytes is calculated using the equation

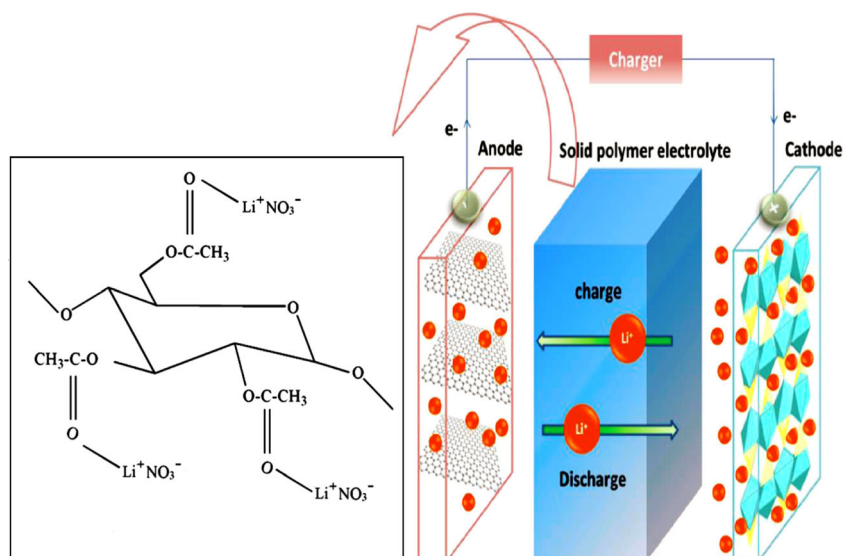
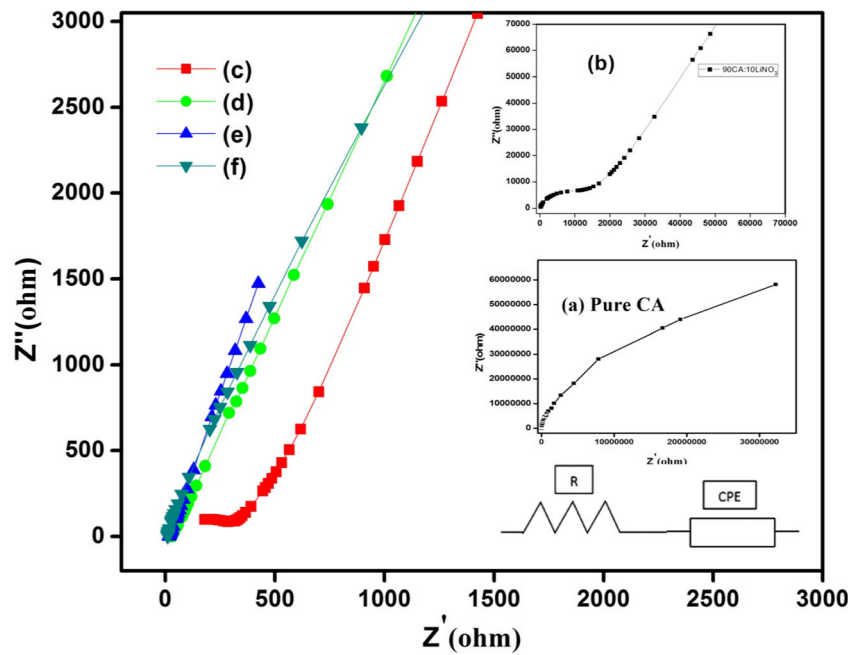
Scheme 1 Conduction mechanism of CA/LiNO₃ complex in lithium ion battery

Fig. 3 Cole-Cole plot for *a* pure CA, *b* 90CA/10LiNO₃, *c* 80CA/20LiNO₃, *d* 70CA/30LiNO₃, *e* 60CA/40LiNO₃, and *f* 50CA/50LiNO₃ BPEs and the corresponding equivalent circuit



$$\sigma = \frac{L}{A \times R_b} \text{ S cm}^{-1} \tag{1}$$

where L is the thickness, R_b is the bulk resistance, and A is the contact area of the electrolyte film. Table 2 indicates the calculated ionic conductivity for different concentration of CA/LiNO₃ BPEs with various temperatures. The highest ionic conductivity of 1.93×10^{-3} S/cm is achieved at room temperature for 50CA/50LiNO₃ BPE, which has greater ionic conductivity than that of pure CA (1.285×10^{-7}). The increase in the ionic conductivity is due to the increase in charge carriers of the electrolyte system. Kingslin et al. reported that the conductivity of 15 wt.% LiNO₃ with PVA/PAN polymer blend reaches a maximum conductivity value of 1.5×10^{-3} S/cm [18]. The present result shows the same order of conductivity with single polymer-salt complex. However, further addition of lithium salt above 50 wt.% causes the electrolyte to be unstable, which is attributed to the formation

of linkage between the salt itself and causing it to recrystallize resulting in the decrease in conductivity [31].

Temperature-dependent conductivity

Figure 4 shows the variation of conductivity as the function of temperature for various concentration of LiNO₃ in the BPEs from room temperature to 70 °C. The conductivity-temperature plots followed an Arrhenius behavior throughout the temperature range. The variation of conductivity (σ) with temperature (T) can be fitted to the relation

$$\sigma = \sigma_0 \exp(-E_a/KT) \tag{2}$$

where σ , σ_0 , E_a , K , and T are the ionic conductivity, pre-exponential factor, activation energy, Boltzmann constant, and absolute temperature, respectively. This can be explained by ion

Table 2 Ionic conductivity and activation energy values of CA/LiNO₃ BPEs for different temperature

Polymer composition (mol%)	$\sigma_{303 \text{ k}}$	$\sigma_{313 \text{ k}}$	$\sigma_{323 \text{ k}}$	$\sigma_{333 \text{ k}}$	$\sigma_{343 \text{ k}}$	Activation energy E_a (eV) at room temperature	Regression value
Pure CA	1.29×10^{-7}	8.42×10^{-6}	2.68×10^{-5}	2.47×10^{-5}	7.86×10^{-5}	1.2	0.90
90CA/10LiNO ₃	1.51×10^{-7}	8.19×10^{-7}	1.09×10^{-6}	1.57×10^{-6}	2.47×10^{-6}	0.56	0.98
80CA/20LiNO ₃	1.02×10^{-5}	2.33×10^{-5}	3.56×10^{-5}	5.99×10^{-4}	9.07×10^{-4}	0.48	0.95
70CA/30LiNO ₃	1.04×10^{-4}	1.9×10^{-4}	2.98×10^{-4}	3.69×10^{-4}	3.78×10^{-4}	0.29	0.94
60CA/40LiNO ₃	2.38×10^{-4}	4.75×10^{-4}	5.67×10^{-4}	6.03×10^{-4}	6.13×10^{-3}	0.19	0.90
50CA/50LiNO ₃	1.93×10^{-3}	2.09×10^{-3}	2.96×10^{-3}	3.50×10^{-3}	3.64×10^{-3}	0.16	0.98

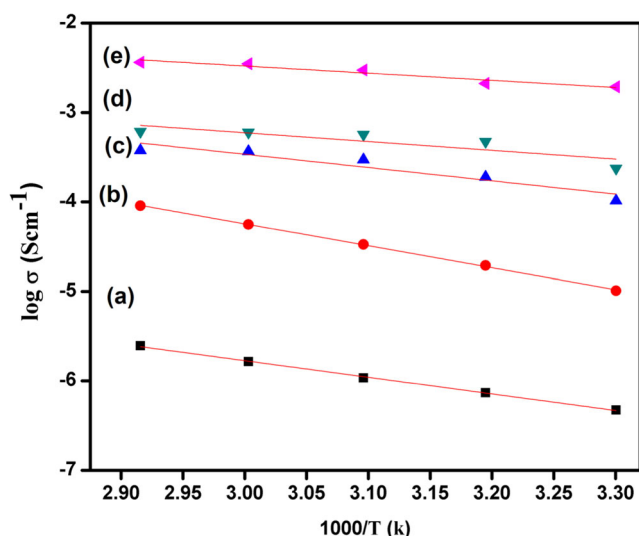


Fig. 4 Temperature dependence ionic conductivity of *a* 90CA/10LiNO₃, *b* 80CA/20LiNO₃, *c* 70CA/30LiNO₃, *d* 60CA/40LiNO₃, and *e* 50CA/50LiNO₃ BPEs

hopping mechanism. As the temperature increases, the conductivity also increases because the vibrational modes of polymer segments increases and gain sufficient energy to push against the hydrostatic pressure, which is imposed by its surrounding atoms and turns to the formation of voids [32]. At the same time, the polymer expands to produce free volume, which leads to create the interaction between the polar group of the polymer backbones and Li⁺ thus promotes the charge carriers to the polymer matrix and enhanced the ionic conductivity [33]. The values of conduction and activation energy as a function of LiNO₃ concentration are listed in Table 2.

Dielectric studies

Relaxation behavior of electrolytes can be implicit from dielectric studies. Dielectric studies in the BPE system help to identify the conductivity behavior.

Figure 5a, b shows the frequency-dependent plot of ϵ' and ϵ'' parts of dielectric permittivity curves. From the graph, it has been observed that ϵ' and ϵ'' increase at low frequencies, which indicates the electrode polarization and space charge effects that confirm the non-debye nature [34]. At high frequencies, the periodic reversal of the applied electric field takes place so rapidly that the mobile ion will not be able to orient them in the field direction resulting it to saturate or decrease the dielectric constant [35]. The higher value for both ϵ' and ϵ'' has been observed for 50CA/50LiNO₃ BPE. The increase in dielectric loss and dielectric constant are due to high charge density. This indicates that the degree of salt dissociation and redissociation of ion aggregates causes the increase in the number of free ion that in turn increases the conductivity of the sample [36].

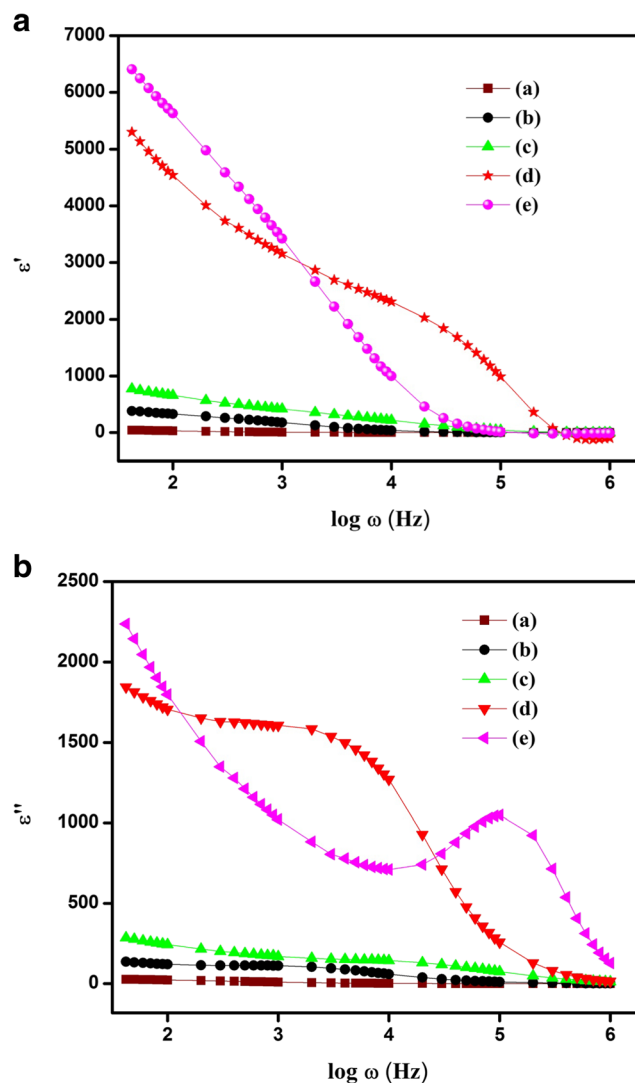


Fig. 5 **a** Frequency dependence of $\epsilon'(\omega)$ of *a* 90CA/10LiNO₃, *b* 80CA/20LiNO₃, *c* 70 CA/30LiNO₃, *d* 60CA/40LiNO₃, and *e* 50CA/50LiNO₃ BPEs. **b** Frequency dependence of $\epsilon''(\omega)$ of *a* 90CA/10LiNO₃, *b* 80CA/20LiNO₃, *c* 70 CA/30LiNO₃, *d* 60CA/40LiNO₃, and *e* 50CA/50LiNO₃ BPEs

Electrochemical stability

Electrochemical stability is an important criterion to investigate the working cell potential of an electrolyte. The sample has been placed between two stainless steel blocking electrodes using 1 mVs⁻¹ scan rate from 0 to 5 V. Figure 6 shows the linear sweep voltammetry of the highest conducting film 50CA/50LiNO₃. The anodic decomposition limit of the polymer electrolyte is considered the voltage at which the current flows through the cells [2]. As seen from the plot of current versus voltage, the electrolyte shows the electrochemical stability window of 4.09 V. The result shows that it could be used for energy storage devices.

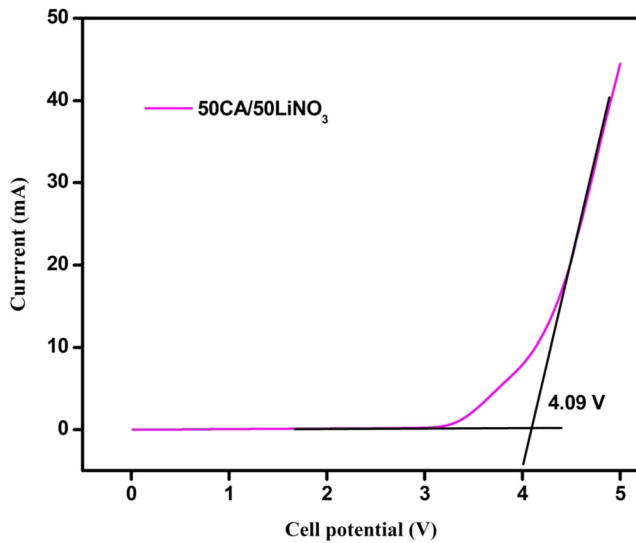


Fig. 6 Linear sweep voltagram of 50CA/50LiNO₃-based BPE

Transference number measurement

Transference number measurement (TNM) has been carried out to investigate the main conducting element in the BPEs using the DC polarization method [37]. The transference number has been calculated using the following formula:

$$t_{ion} = (I_i - I_f) / I_i \tag{3}$$

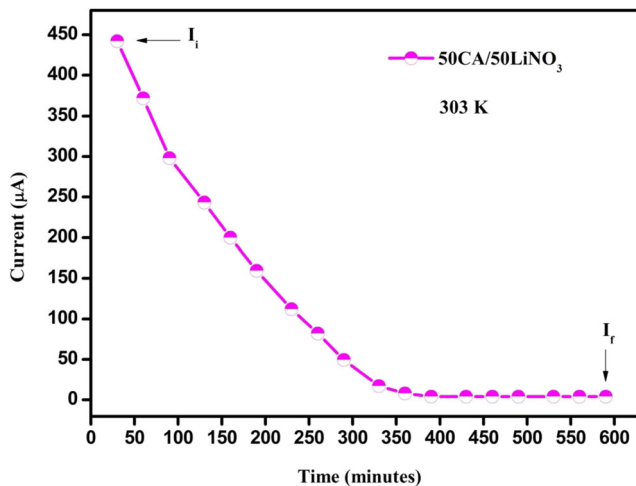


Fig. 7 Polarization current vs time plot for highest conducting BPE 50CA/50LiNO₃

$$t_{elec} = I_f / I_i \tag{4}$$

where, I_i is the initial current and I_f is the final current. In this method, fixed dc voltage of 1.0 V has been applied to the cell stainless steel/50CA/50LiNO₃/stainless steel. The plot of current versus time for the highest conducting film is shown in Fig. 7. The initial total current (I_i) has been found to decrease with time, which is due to the depletion of ionic species in the electrolyte and become constant in the fully depleted situation. At the steady state, the cell is polarized and the current flows because of electron migration across the electrolyte and interfaces. The values of ionic transference number are in the range of 0.97–0.99, which is close to unity. The ionic currents through an ion-blocking electrode fall rapidly with time if the electrolyte is primarily ionic. These results clearly revealed that Li⁺ ions from LiNO₃ complex with CA become an almost perfect ionic conductor and electronic contribution to the total current is negligible.

The diffusion coefficients of cations and anions of 60CA/40LiNO₃, 50CA/50LiNO₃, and 40CA/60 LiNO₃ were calculated using the following equations [38],

$$D = D_+ + D_- = \frac{KT\sigma}{ne^2} \tag{5}$$

$$t_+ = \frac{D_+}{D_+ - D_-} \tag{6}$$

The ionic mobility of cations and anions of all the samples is calculated using the following equations.

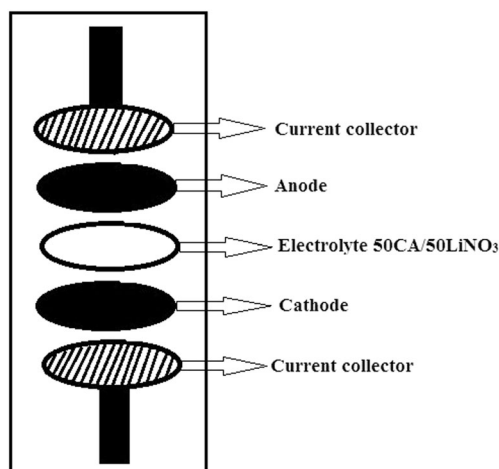
$$\mu = \mu_+ + \mu_- = \frac{\sigma}{ne} \tag{7}$$

$$t_+ = \frac{\mu_+}{\mu_+ + \mu_-} \tag{8}$$

where, e is the charge of the electron, k is the Boltzmann constant, T is the absolute temperature, n is the number of charge carriers stoichiometrically related to the salt composition, μ_+ and μ_- are the ionic mobility of cation and anion, respectively, and D_+ and D_- are the diffusion coefficients of cation and anion, respectively. Resulting data are shown in Table 3, which shows that the cation mobility of μ_+ is greater than the anion mobility μ_- . If the conductivity decreases, the mobility also decreases and vice versa. The same behavior is reflected for D_+ .

Table 3 Ionic mobility and diffusion coefficient of cations and anions of BPEs

Polymer composition (mol%)	n (cm ⁻³)	t_{ion}	D_+ (cm ² s ⁻¹)	D_- (cm ² s ⁻¹)	μ_+ (cm ² V ⁻¹ s ⁻¹)	μ_- (cm ² V ⁻¹ s ⁻¹)
60CA/40LiNO ₃	4.55×10^{21}	0.98	1.52×10^{-8}	5×10^{-10}	4.91×10^{-7}	0.16×10^{-7}
50CA/50LiNO ₃	5.23×10^{21}	0.99	1.25×10^{-7}	2×10^{-9}	5.01×10^{-6}	0.06×10^{-8}
40CA/60LiNO ₃	8.04×10^{21}	0.98	1.66×10^{-8}	4×10^{-10}	6.38×10^{-7}	1.3×10^{-8}



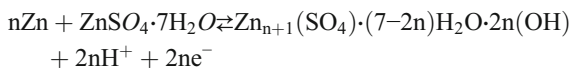
Scheme 2 Schematic diagram of battery holder

Fabrication and characterization of lithium ion battery

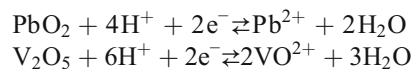
A primary lithium ion battery with the highest conducting membrane 50CA/50LiNO₃ has been constructed with the configuration Zn + ZnSO₄·7H₂O/50CA/50LiNO₃/PbO₂ + V₂O₅. The procedure of fabrication of battery has been reported in literature [27]. Graphite has been added to the electrode to introduce the electronic conductivity. The schematic diagram of fabricated battery was shown in Scheme 2.

The anode and cathode reactions are given below.

Anode reaction



Cathode reaction



The open circuit voltage (OCV) of the constructed lithium ion battery has been monitored for 28 h and plotted against time as shown in Fig. 8a. The OCV of the cell at room temperature shows the initial voltage of 1.8 V, dropping to 1.5 V in the first 20 h of assembly. The discharge profile of the constructed lithium ion battery has been shown in Fig. 8b by connecting it to the external load of 1 MΩ. The load voltage of the battery drops to 1.5 from 1.8 V in 15 h of assembly. The initial drop in the voltage of the cell is attributed to the polarization effect at the electrode/electrolyte interface [39]. Similarly, lithium primary battery for 92.5PVA/7.5PAN/30 wt.% LiBr polymer electrolyte has been demonstrated by

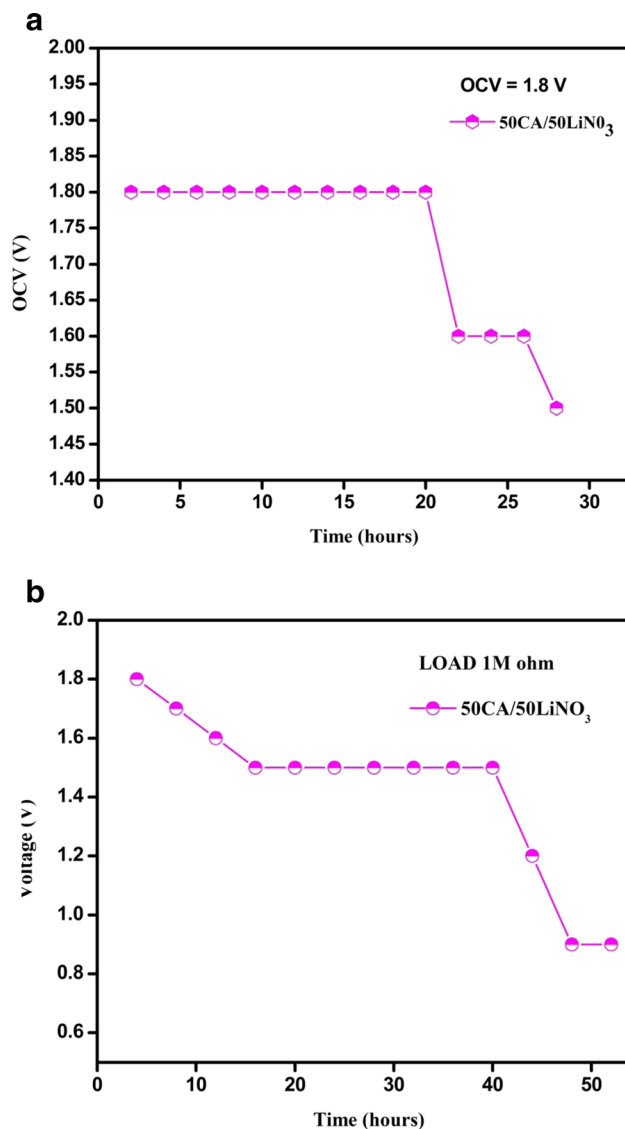


Fig. 8 a Open circuit voltage as a function of time for 50CA/50LiNO₃ BPE. b Discharge curve of the cell using 1 MΩ for 50CA/50LiNO₃ BPE

Kingslin et al. [40]. The OCV and load voltage of CA-based polymer electrolyte achieve better performance than blended polymer electrolytes. The OCV and discharge time for the plateau region and other cell parameters for this cell are listed in Table 4. From the battery application, it is evident that this battery is suited for low current density applications.

Table 4 Important cell parameters

Cell area (cm ²)	0.895
Cell weight (g)	1.284
Effective cell diameter (cm)	1
Cell thickness (cm)	0.288
Open circuit voltage (OCV; V)	1.8
Discharge time for plateau region (h)	25

Conclusion

Solid biopolymer electrolytes based on CA and LiNO₃ has been successfully prepared using solution-casting technique. XRD analysis revealed that the inclusion of LiNO₃ alter the crystallinity of CA. The strong complex interaction occurs between the oxygen group of CA and lithium ion has been observed from FTIR spectra. EIS analysis confirmed that charge carriers in the system 50CA/50LiNO₃ reaches the ionic conductivity 1.93×10^{-3} S/cm at room temperature. The temperature-dependent ionic conductivity of these highest conducting BPE obeys the Arrhenius relationship with low activation energy. Ionic transference number (t^+) measurement reveals that the conducting species are predominantly lithium ions. The electrochemical stability window for 50CA/50LiNO₃ proved that the SPE is suitable to be applied in electrochemical devices. The high ionic conductivity BPE has also been tested for primary battery application, and its parameters are reported. The result in the present study suggested that CA/LiNO₃ BPE is one of the capable electrolytes for lithium battery application.

References

- Changyu T, Ken H, Qiang F, Pulickel MA, Haleh A (2012) High ion conducting polymer nanocomposite electrolytes using hybrid nanofillers. *Nano Lett* 12:1152–1156
- TianKhoon L, Ataollahi N, Hassan NH, Ahmad A (2015) Studies of porous solid polymeric electrolytes based on poly(vinylidene fluoride) and poly (methyl methacrylate) grafted natural rubber for applications in electrochemical devices. *J Solid State Electrochem* 1:203–213
- Polu AR, Rhee H-W, Kim DK (2015) New solid polymer electrolytes (PEO20–LiTDI–SN) for lithium batteries: structural, thermal and ionic conductivity studies. *J Mater Sci Mater Electron* 11:8548–8554
- Lin CW, Hung CL, Venkateswarlu M, Hwang BJ (2005) Influence of TiO₂ nano-particles on the transport properties of composite polymer electrolyte for lithium-ion batteries. *J Power Sources* 146:397–401
- Ramesh S, Liew C-W, Arof AK (2011) Ion conducting corn starch biopolymer electrolytes doped with ionic liquid 1-butyl-3-methylimidazolium hexafluorophosphate. *J Non-Cryst Solids* 357:3654–3660
- Osman Z, Ibrahim Z, Arof AK (2001) Conductivity enhancement due to ion dissociation in plasticized chitosan based polymer electrolytes. *Carbohydr Polym* 44:167–173
- Liew C-W, Ramesh S (2013) Studies on ionic liquid-based corn starch biopolymer electrolytes coupling with high ionic transport number. *Cellulose* 20:3227–3237
- Raphael E, Avellaneda CO, Manzolli B, Pawlicka A (2010) Agar based films for application as polymer electrolytes. *Electrochim Acta* 55:1455–1459
- Shamsudin IJ, Ahmad A, Hassan N, Kaddami H (2015) Bifunctional ionic liquid in conductive biopolymer based on chitosan for electrochemical devices application. *Solid State Ionics* 278:11–19
- Samir MA, Chazeau L, Alloin F, Cavaillé J-Y, Dufresne A, Sanchez J-Y (2005) POE-based nanocomposite polymer electrolytes reinforced with cellulose whiskers. *Electrochim Acta* 50:3897–3903
- Monisha S, Selvasekarapandian S, Mathavan T, Milton Franklin Benial A, Manoharan S, Karthikeyan S (2016) Preparation and characterization of biopolymer electrolyte based on cellulose acetate for potential applications in energy storage devices. *J Mater Sci Mater Electron*. doi:10.1007/s10854-016-4971-x
- Ramesh S, Shanthi R, Morris E (2012) Plasticizing effect of 1-allyl-3-methylimidazolium chloride in cellulose acetate based polymer electrolytes. *Carbohydr Polym* 87:2624–2629
- Ramesh S, Shanthi R, Morris E (2013) Characterization of conducting cellulose acetate based polymer electrolytes doped with “green” ionic mixture. *Carbohydrate Polymer* 9:14–21
- Shukur MF (2015) Characterization of ion conducting solid biopolymer electrolytes based on starch-chitosan blend and application in electrochemical devices. Thesis dissertation, University of Malaya, Malaysia
- Amran NNA, Manan NSA, Kadir MFZ (2016) The effect of LiCF₃SO₃ on the complexation with potato starch-chitosan blend polymer electrolytes. *Ionics*. doi:10.1007/s11581-016-1684-3
- Abidin SZZ, Ali AMM, Hassan OH, Yahya MZA (2013) Electrochemical studies on cellulose acetate-LiBOB polymer gel electrolytes. *Int J Electrochem Sci* 8:7320–7326
- Selvakumar M, Krishna Bhat D (2008) LiClO₄ doped cellulose acetate as biodegradable polymer electrolyte for supercapacitors. *J Appl Polym Sci* 110:594–602
- Kingslin Mary Genova F, Selvasekarapandian S, Karthikeyan S, Vijaya N, Sivadevi S, Sanjeeviraja C (2015) Lithium ion-conducting blend polymer electrolyte based on PVA-PAN doped with lithium nitrate. *Polymer Plastic Technology and Engineering* 1:25–35
- Ravi M, Song S, Wang J, Wang T, Nadimicherla R (2015) Ionic liquid incorporated biodegradable gel polymer electrolyte for lithium ion battery applications. *J Mater Sci Mater Electron* 2:1370–1377
- Samsudin AS, Khairul WM, Isa MIN (2012) Characterization on the potential of carboxymethylcellulose for application as proton conducting biopolymer electrolytes. *J Non-Cryst Solids* 358:1104–1112
- Pradhan DK, Choudhary RNP, Samantaray BK (2008) Studies of dielectric relaxation and AC conductivity behavior of plasticized polymer nanocomposite electrolytes. *Int J Electrochem Sci* 3:597–608
- Su'ait MS, Ahmad A, Badri KH, Mohamed NS, Rahman MYA, Azanza Ricardo CL, Scardi P (2013) The potential of polyurethane bio-based solid polymer electrolyte for photoelectrochemical cell application. *Int J Hydrog Energy* 6:3005–3017
- Ataollahi N, Ahmad A, Hamzah H, Rahman MYA, Mohamed NS (2013) Ionic conduction of blend poly (vinylidene fluoride-hexafluoro propylene) and poly (methyl methacrylate)-grafted natural rubber based solid polymer electrolyte. *Int J Electrochem Sci* 8:7875–7884
- Sulaiman M, Rahman AA, Mohamed NS (2015) Effect of water-based sol gel method on structural, thermal and conductivity properties of LiNO₃–Al₂O₃ composite solid electrolytes. *Arab J Chem*. doi:10.1016/j.arabjc.2015.04.031
- Eswaraiah V, Sankaranarayanan V, Ramaprabhu S (2001) Inorganic nanotubes reinforced polyvinylidene fluoride composites as low-cost electromagnetic interference shielding materials. *Res Lett* 6:137–147
- Shamsudin IJ, Ahmad A, Hassan NH, Kaddami H (2016) Biopolymer electrolytes based on carboxymethyl–carrageenan and imidazolium ionic liquid. *Ionics* 6:841–851
- Sikkanthar S, Karthikeyan S, Selvasekarapandian S, Vinoth Pandi D, Nithya S, Sanjeeviraja C (2015) Electrical conductivity characterization of polyacrylonitrile-ammonium bromide polymer electrolyte system. *J Solid State Electrochem* 19:987–999
- Watanabe M, Sanui K, Ogata N, Kobayashi T, Ohbaki Z (1985) Ionic conductivity and mobility in network polymers from poly(propylene oxide) containing lithium perchlorate. *J Appl Phys* 57:123
- Boukamp BA (1986a) *Solid State Ionics* 20:301
- Boukamp BA (1986b) *Solid State Ionics* 18(19):136

31. Ahn JH, Wang GX, Liu HK, Dou SX (2003) Nanoparticle dispersed in PEO polymer electrolytes for Li batteries. *J Power Sources* 119–121: 422–426
32. Rajendran S, Sivakumar M, Subadevi R (2004) Investigations on the effect of various plasticizers in PVA-PMMA solid polymer electrolytes. *Mater Lett* 58:641–649
33. Aravindan V, Vickraman P (2007) A novel gel electrolyte with lithium difluoro(oxalate)borate salt and Sb_2O_3 nanoparticles for lithium ion batteries. *Solid State Sci* 9:1069–1073
34. Qian X, Gu N, Cheng Z, Yang X, Wang E, Dong S (2001) Impedance study of (PEO) 10 $LiClO_4$ - Al_2O_3 composite polymer electrolyte with blocking electrodes. *Electrochim Acta* 46:1829–1836
35. Adachi K, Urakawa O (2002) Dielectric study of concentration fluctuations in concentrated polymer solutions. *J Non-Crystalline Solids* 667:307–310
36. Shastry S, Rao KJ (1991) AC conductivity and dielectric relaxation studies in AgI-based fast ion conducting glasses. *Solid State Ionics* 44: 187–198
37. Wagner JB, Wagner CJ (1957) Electrical conductivity measurements on cuprous halides. *Chem Rev* 26:1597
38. Winnie T, Arof AK (2006) Transport properties of hexanoyl chitosan-based gel electrolyte. *Ionics* 12:149–152
39. Subba Reddy CV, Sharma AK, Narasimha Rao VVR (2003) Conductivity and discharge characteristics of polyblend (PVP+ PVA + KIO_3) electrolyte. *J Power Sources* 114:338–345
40. Kingslin Mary Genova F, Selvasekarapandian S, Karthikeyan S, Vijaya N, Pradeepa R, Sivadevi S (2015) Study on blend polymer (PVA-PAN) doped with lithium bromide. *Polymer Science Ser A* 57:851–862